

Dissipation effects in the ratchetlike Fermi acceleration

Cesar Manchein and Marcus W. Beims^{1,*}

¹*Departamento de Física, Universidade Federal do Paraná, 81531-980 Curitiba, PR, Brazil*

(Dated: May 29, 2022)

Ac driven asymmetric pulses can be used to control the Fermi acceleration between three different motions, **A** : the *accelerated* mode; **D** : the *decelerated* mode and **H** : the *hyperaccelerated* mode. In this work we show that dissipation strongly affects the particles velocity, reducing the possibility for an accurate control of the dynamics. The saturation time, where the mean velocity starts to be constant due to dissipation, decays with a power law $\sim \gamma^{-\beta}$, where γ is the dissipation parameter and β is close to 1. The value of the saturated mean velocity also decays with a power law with exponent $\beta \sim 0.6$ for the case **H**, and $\beta \sim 0.3$ for the case **A**. In the case **D** this velocity is almost constant for small dissipations.

PACS numbers: 05.45.-a, 05.10.-a

Keywords: Fermi acceleration, Control, Ratchet, Dissipation

Fermi acceleration is a topic which got attention in various areas of physics, ranging from nonlinear physics [1, 2, 3, 4, 5, 6, 7, 8], atom optics [9, 10, 11], plasma physics [12, 13] to astrophysics [14, 15, 16]. After the first model proposed by Fermi [17], essentially two different versions became common in the literature. In the first one, the Fermi-Ulam (FU) model, a bouncing particle moves between a fixed surface and a parallel oscillating surface [18]. In this case the regular islands in the phase space prevent the Fermi acceleration. A simplified version of this model was proposed to improve simulations [1], called the static wall model. It essentially ignores the displacement of the moving wall but keeps the information for the momentum transfer as the wall was oscillating. The dynamics of the static model was studied in different aspects [1, 3, 4, 5] and for different models [6], and the relevant result for the purpose of the present work is that invariant curves in the phase space, found for higher velocities, prevent the particle to increase its kinetic energy without bounds. Recently the hopping wall approximation was proposed [7, 8] which takes into account the effect of the wall displacement, and allows the analytical estimation of the particle mean velocity. Compared to the simplified static model, the particle acceleration is enhanced. The second kind of Fermi accelerated model was proposed in 1977 by Pustyl'nikov [19], who considered a particle on a periodically oscillating horizontal surface in the presence of a gravitational field. Different from the FU model, for some initial conditions and control parameters the particle energy can grow indefinitely.

In this paper we analyze the effect of dissipation in the simplified FU model when an ac driven asymmetric pulse controls the Fermi acceleration (deceleration) [20]. Small dissipation is inevitable in real systems and its influence on the dynamics of conservative systems is of great interest [21, 22, 23] since elliptic periodic orbits become small sinks and attractors start to exist [24, 25]. In the context of Fermi models dissipation effects have been inserted in two ways: frictional force [26] and inelastic collisions at the walls [27, 28, 29]. Here we use the second approach and the pulse is a *deformed* sawtooth driving law for the moving wall. This Ratchetlike pulse differs from the ac driven asymmetric pulses (*symmetric* sawtooth) used for the Fermi acceleration in the early work of Lichtenberg *et. al* [1] and proposed recently to control the motion of magnetic flux quanta [30] and to analyse the relative efficiency of mechanism leading to increased acceleration in the hopping wall approximation [8]. In the simplified Fermi model [1] the particle is free to move between the elastic impacts with the walls. Consider that the moving wall oscillates between two extrema with amplitude v_0 . The gravitational force is considered zero. The system is described by a two-dimensional map $M_{1(2)}(V_n, \phi_n) = (V_{n+1}, \phi_{n+1})$ which gives, respectively, the velocity of the particle, and the phase of the moving wall, immediately after the particle suffers a collision with the wall. Considering dimensionless variables the dissipative FU map with the *deformed* sawtooth wall is written as

$$M_1 : \begin{cases} V_{n+1} = \left| (1 - \gamma)V_n + \frac{v_0}{\eta_1}(\phi_n - \eta_1) \right|, \\ \phi_{n+1} = \phi_n + \mu \frac{(\eta_1 + \eta_2)}{V_{n+1}} \quad \text{mod } (\eta_1 + \eta_2), \end{cases} \quad (1)$$

for $\phi_n < \eta_1$, and

$$M_2 : \begin{cases} V_{n+1} = \left| (1 - \gamma)V_n + \frac{v_0}{\eta_2}(\phi_n - \eta_1) \right|, \\ \phi_{n+1} = \phi_n + \mu \frac{(\eta_1 + \eta_2)}{V_{n+1}} \quad \text{mod } (\eta_1 + \eta_2), \end{cases} \quad (2)$$

for $\phi_n \geq \eta_1$, where n is the iteration number and μ is the maximum distance between the walls. For $\gamma \neq 0$ we have dissipation effects. Since in this simplified model the displacement of the moving wall is ignored, the modulus function is used to avoid errors due to successive collisions which may occur in the original model. In other words, if after a collision with the wall the particle continues to have a negative velocity (a successive collision will occur in the original model), the particle moves beyond the wall. The modulus for the velocity injects the particle back and fixes the problem.

The time asymmetry of the oscillating wall in Eqs. (1) and (2) is controlled by varying the parameters (η_1, η_2) . The *deformed* sawtooth (Ratchetlike) is obtained when $\eta_1 \neq \eta_2$. Figures 1(a)-(c) show the time behaviour of the oscillating

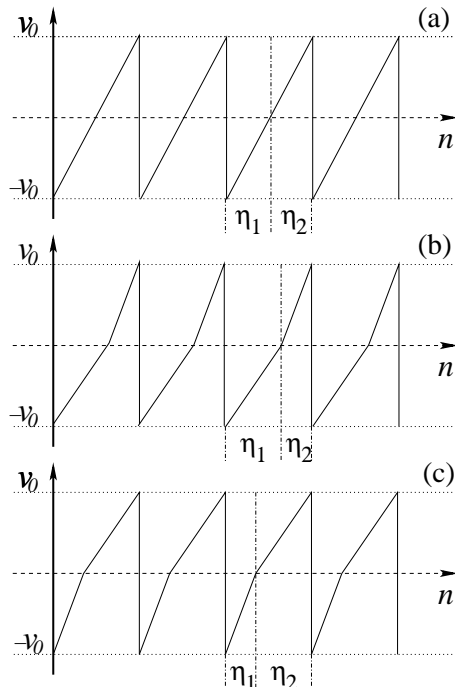


FIG. 1: (a)-(c) The shape of the pulses used in the simulations. The deformed sawtooth effect is obtained when $\Delta\eta = \eta_2 - \eta_1 \neq 0.0$. For (a) $\Delta\eta = 0$ we have the symmetric accelerated case **A**, (b) $\Delta\eta < 0$ we have the deformed decelerated case **D** and (c) $\Delta\eta > 0$ the deformed hyperaccelerated case **H**.

wall (the pulse) for different values of the asymmetry $\Delta\eta = \eta_2 - \eta_1$. The deformed sawtooth pulse is obtained when $\Delta\eta \neq 0.0$. Such pulses can be easily obtained from pulse generators. For the case of no dissipation three different motions were obtained and controlled [20]. They are **A**: for $\Delta\eta = 0$ (symmetric sawtooth) the *accelerated* case [see Fig. 2(a)]; **D**: for $\Delta\eta < 0$ (asymmetric sawtooth) the *decelerated* case [Fig. 3(a)]; and **H**: for $\Delta\eta > 0$ (asymmetric sawtooth) the *hyperaccelerated* case [Fig. 4(a)]. This classification, different from [31], is based on how fast the average velocity grows or decreases. At next we discuss separately the effects of dissipation in each case. To do this we show the corresponding phase space dynamics and determine the mean particles velocity at a given time n from

$$\langle V \rangle(n) = \frac{1}{n+1} \sum_{i=0}^n \frac{1}{\xi} \sum_{j=1}^{\xi} V_{n,j}, \quad (3)$$

where the index i refers to the i th iteration of the sample j , and ξ is the number of initial conditions. We iterate the map (1) or (2) for times $n = 1 \times 10^8$ and 3000 initial conditions in the interval $0 < \phi \leq \eta_1 + \eta_2$ and $0 \leq V \leq 10^{-3}$.

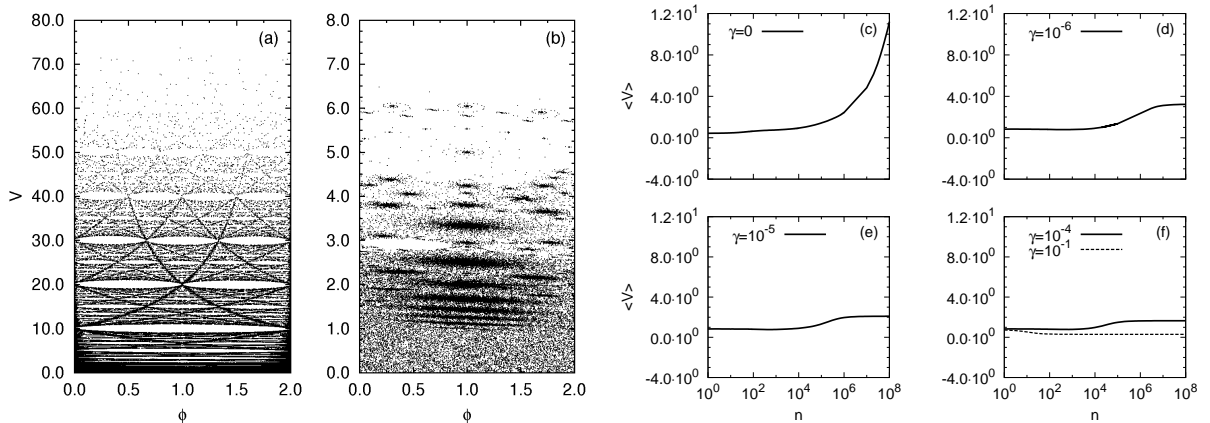


FIG. 2: Evolution of 500 chaotic orbits on the phase space $V \times \phi$ for the parameters $\mu = 10$, $v_0 = 0.2$ for case **A** ($\Delta\eta = 0.0$, $\eta_1 = \eta_2 = 1.00$). For Fig. (a) $\gamma = 0.0$ and (b) $\gamma = 10^{-6}$. The mean values of the velocity, calculated over 3000 trajectories, are shown in (c)-(f) and are related to the cases $\gamma = 0.0, 10^{-6}, 10^{-5}, 10^{-4}, 10^{-1}$.

First we consider the accelerated mode which is similar to the simplified model studied by Lichtenberg and Lieberman [1, 2], where the harmonic force was considered. This case is shown in Fig. 2. As the particle velocity increases, regular islands are observed and $\langle V \rangle$ increases slowly until ~ 10 [Fig. 2(a) and (c)]. The regular islands prevent the particle velocity to increase very fast. We mention that all initial conditions start inside the chaotic region at low velocities. The growth rate of $\langle V \rangle$ depends on the number of regular islands inside the phase space. For very small dissipations ($\gamma = 10^{-6}$) the regular islands are transformed into sinks, as can be observed by comparing Fig. 2(a) and Fig. 2(b) (observe the dark regions), and attract the chaotic trajectories which pass nearby. As a consequence the mean velocity cannot increase as before (compare Fig. 2(c) and (d)). This effect increases for higher values of the dissipation parameter, as can be observed in Figs. 2(e)-(f). Therefore in case **A** the dissipation decreases the mean velocity (to a constant plateau) for any values of γ when compared to the non-dissipative case. There are two additional information we can get from Figs. 2(d)-(f), the saturation time (t_s), where the mean velocity starts to be constant in time and the saturated mean velocity (v_s). Plotting both quantities as a function of γ in the interval $10^{-6} \leq \gamma \leq 10^{-1}$ we obtain the decay $t_c \sim \gamma^{-1.0}$ and $v_c \sim \gamma^{-0.3}$.

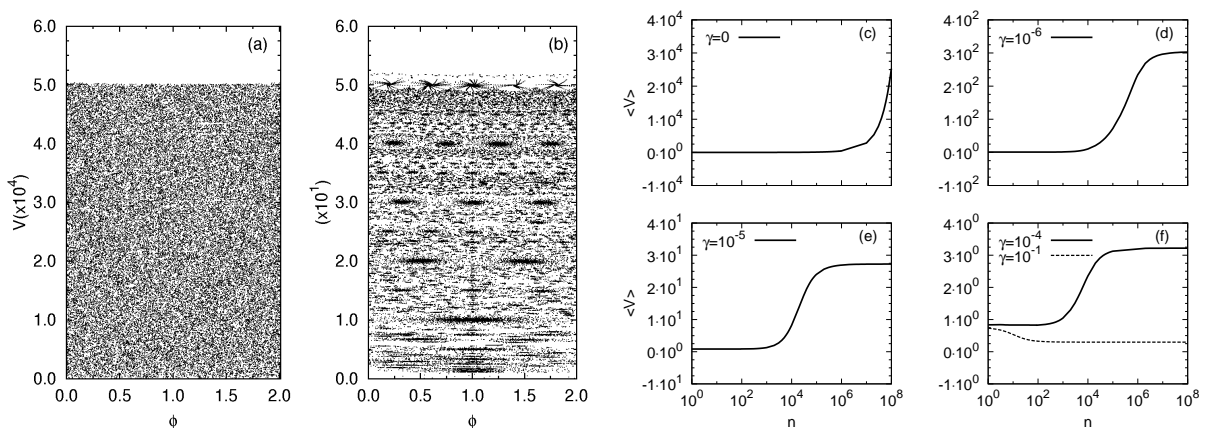


FIG. 3: Evolution of 500 chaotic orbits on the phase space $V \times \phi$ for the parameters $\mu = 10$, $v_0 = 0.2$ for case **H** ($\Delta\eta = 0.01$, $\eta_1 = 1.00$, $\eta_2 = 1.01$). For Fig. (a) $\gamma = 0.0$ and (b) $\gamma = 10^{-6}$. The mean values of the velocity, calculated over 3000 trajectories are shown in (c)-(f) and are related to the cases $\gamma = 0.0, 10^{-6}, 10^{-5}, 10^{-4}, 10^{-1}$.

The second case to discuss is the dissipation in the *hyperaccelerated* case **H** [see Fig. 3(a)]. For a very small asymmetry $\Delta\eta = 0.01$ the phase space is totally filled and no regular islands are observed [Fig. 3(a)]. As shown in [20], the Lyapunov exponents approach zero for this case. The corresponding $\langle V \rangle$ increases very fast until $\langle V \rangle \sim 3 \times 10^4$ [see

Fig. 3(c)], showing that the accelerated mode is enhanced when compared to the case **A**. By adding small dissipation ($\gamma = 10^{-6}$) into the system we observe in Fig. 3(b) that again many sinks appear. In this case however, since no regular islands were observed for $\gamma = 0$, we are not able to relate the sinks to regular islands. On the other hand, we can say that the dissipation is able to find attracting points which were not visible in the conservative limit. Also here small dissipation prevents the hyperacceleration of particles. The mean particles velocity also decreases (to a constant value) due to the small sinks which appear in the phase space shown in Fig. 3(b). For higher values of the dissipation parameter the maximal mean velocity decreases. Observe Fig. 3(d)-(f) for $\gamma = 0.0, 10^{-6}, 10^{-5}, 10^{-4}, 10^{-1}$. For the hyperaccelerated case we found that the saturated quantities decay like $t_c \sim \gamma^{-1.1}$ and $v_c \sim \gamma^{-0.6}$.

Now we discuss the decelerated case **D** ($\Delta\eta = -0.01$). Here many regular islands appear in phase space [see Fig. 4(a)] which again prevent the acceleration to increase without bounds, as in case **A**. The regular islands are very large so that the maximal instantaneous velocity is around ~ 2.5 , while for case **A** it was ~ 70.0 . The corresponding $\langle V \rangle$ remains here almost constant [see Fig. 4(c)]. As in the other cases, when small dissipation is added ($\gamma = 10^{-6}$) into the system, regular islands are transformed into sinks. However here the mean velocity *increases* [see Fig. 4(d)]. This increasing in the mean velocity is easy to explain. Since the first (from below) four islands from the conservative

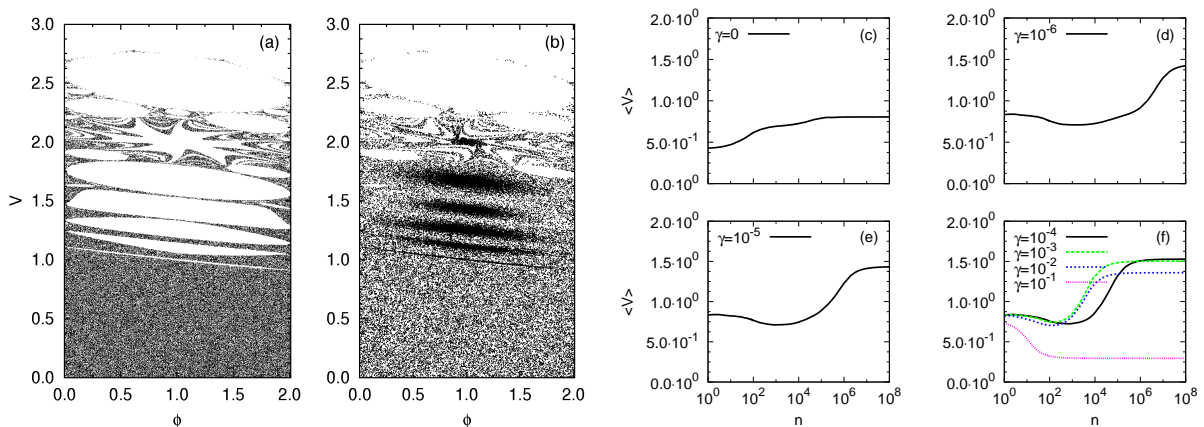


FIG. 4: Evolution of 500 chaotic orbits on the phase space $V \times \phi$ for the parameters $\mu = 10$, $v_0 = 0.2$ for case **D** ($\Delta\eta = -0.01$, $\eta_1 = 1.01$, $\eta_2 = 1.00$). For Fig. (a) $\gamma = 0.0$ and (b) $\gamma = 10^{-6}$. The mean values of the velocity, calculated over 3000 trajectories, are shown in (c)-(f) and are related to the cases $\gamma = 0.0, 10^{-6}, 10^{-5}, 10^{-4}, 10^{-3}, 10^{-2}, 10^{-1}$.

system are very large (see Fig. 4(a)), almost all initial conditions cannot reach velocities higher than ~ 1.1 . It is a kind of upper partial barrier for the velocities. However, when small dissipation is added, these four islands are transformed into sinks so that the chaotic trajectories can penetrate the islands and the upper barrier does not exist anymore. This makes the mean velocity to increase because the position of the sinks are higher (in velocity) than the upper barrier. Such increase in the mean velocity when dissipation is present was also observed in [25]. For the decelerated case we found for the saturated time $t_c \sim \gamma^{-1.2}$ while v_c is constant in the interval $10^{-6} \leq \gamma \leq 10^{-2}$ and decreases for $\gamma = 0.1$.

To conclude, for a long time the Fermi acceleration has been studied in different models and applications [1, 2, 3, 4, 5, 6, 7, 8, 9, 10, 11, 12, 13, 14, 15, 16, 17, 18, 19, 30], but just recently [20] a deformed sawtooth (Ratchetlike) pulse was proposed to control the Fermi de(acceleration). Changing the asymmetry parameter from the Ratchetlike pulse it was possible to get Fermi hyperacceleration and deceleration. By switching the pulse between hyperacceleration and deceleration modes an accurate control of the particles velocity was achieved. Beside the remarkable control of velocities obtained in the dissipation free problem, we observe here that dissipation effects transform regular islands into sinks, change the mean velocity and reduce the ability to control accurately the particle dynamics. The saturation time decays with a power law $t_c \sim \gamma^{-\beta}$, where β is close to 1.0 (± 0.01) for all considered cases. On the other hand, the saturated mean velocity also obeys the power law decay, but with exponents $\beta \sim 0.6$ for the case **H**, and $\beta \sim 0.3$ for the case **A**. In the decelerated case the saturated velocity is almost constant for small dissipations. Our results motivate further analysis related to the control of Fermi de(acceleration) for larger Ratchetlike asymmetries of the ac driven pulse in the presence of dissipation [32] and in the hopping wall approximation. In the later case we expect to obtain a better efficiency to control the particles velocity since the the energy gain per collision is not underestimated as in the present model. In addition, it would be interesting to analyse the implementation of the Ratchetlike ac driven pulse applied to the walls of quasi one-dimensional billiards which are coupled to thermal baths at different

temperatures. In such cases it is desirable to optimize and achieve the control of directed heat conduction [33], which could lead to an important increase of the thermal efficiency in physical devices such as rectifiers and thermal transistors [34].

ACKNOWLEDGMENTS

The authors thank CNPq and FINEP (under project CTINFRA-1) for financial support.

* E-mail address: mbeims@fisica.ufpr.br

- [1] M. A. Lieberman and A. J. Lichtenberg, *Phys. Rev. A* **5**, 1852 (1972).
- [2] A. J. Lichtenberg and M. A. Lieberman, *Regular and Chaotic Dynamics* (Springer-Verlag, 1992).
- [3] E. D. Leonel, J. K. L. da Silva, and S. O. Kamphorst, *Physica A* **331**, 435 (2004).
- [4] E. D. Leonel, P. V. E. McClintock, and J. K. L. da Silva, *Phys. Rev. Lett.* **93**, 014101 (2004).
- [5] E. D. Leonel and P. V. E. McClintock, *J. Phys. A* **38**, 823 (2005).
- [6] R. E. de Carvalho, F. C. Souza, and E. D. Leonel, *Phys. Rev. E* **73**, 066229 (2006).
- [7] A. K. Karlis, P. K. Papachristou, F. K. Diakonou, V. Constantoudis, and P. Schmelcher, *Phys. Rev. Lett.* **97**, 194102 (2006).
- [8] A. K. Karlis, P. K. Papachristou, F. K. Diakonou, V. Constantoudis, and P. Schmelcher, *Phys. Rev. E* **76**, 016214 (2007).
- [9] A. Steane, P. Szriftgiser, P. Desbiolles, and J. Dalibard, *Phys. Rev. Lett.* **74**, 4972 (1995).
- [10] F. Saif, I. Bialynicki-Birula, M. Fortunato, and W. P. Schleich, *Phys. Rev. A* **58**, 4779 (1998).
- [11] F. Saif, *Phys. Rep.* **419**, 207 (2005).
- [12] A. V. Milovanov and L. M. Zeleny, *Phys. Rev. E* **64**, 052101 (2001).
- [13] G. Michalek, M. Ostrowski, and R. Schickeiser, *Sol. Phys.* **184**, 339 (2001).
- [14] A. Veltri and V. Carbone, *Phys. Rev. Lett.* **92**, 143901 (2004).
- [15] K. Kobayakawa, Y. S. Honda, and T. Tamura, *Phys. Rev. D* **66**, 083004 (02).
- [16] M. A. Malkov, *Phys. Rev. E* **58**, 4911 (1998).
- [17] E. Fermi, *Phys. Rev.* **75**, 1169 (1949).
- [18] S. M. Ulam (University of California Press, Berkely, 1961), vol. 3.
- [19] L. D. Pustyl'nikov, *Trudy Moskov. Mat. Obsc. Tom* **34**, 1 (1977)(*Trans. Moscow. Math. Soc.* **2**, 1 (1978)).
- [20] C. Manchein and M. W. Beims, *J. Comp. Int. Science* **1**, 99 (2009).
- [21] Y.-C. Lai and C. Grebogi, *Phys. Rev. E* **54**, 4667 (1996).
- [22] P. C. Rech, M. W. Beims, and J. A. C. Gallas, *Phys. Rev. E* **71**, 17207 (2005).
- [23] C. Manchein, J. Rosa, and M. W. Beims, *Physica D*, arXiv:0905.4940 (2009).
- [24] U. Feudel, C. Grebogi, B. R. Hunt, and J. A. Yorke, *Phys. Rev. E* **54**, 71 (1996).
- [25] R. E. de Carvalho and C. V. Abud, *Phys. Rev. E* **77**, 036204 (2008).
- [26] D. F. Tavares, *Braz. J. Phys.* **38**, 58 (2008).
- [27] E. D. Leonel and R. E. de Carvalho, *Phys. Lett. A* **364**, 475 (2007).
- [28] A. L. P. Livorati, D. G. Ladeira, and E. D. Leonel, *Phys. Rev. E* **78**, 056205 (2008).
- [29] D. G. Ladeira and E. D. Leonel, *Chaos* **17**, 013119 (2007).
- [30] D. Cole, S. Bending, S. Savell'ev, A. Grigorenko, T. Tamegai, and F. Nori, *Nature Materials* **5**, 305 (2006).
- [31] A. Loskutov, *Physics-Uspekhi* **50**, 939 (2007).
- [32] C. Manchein and M. W. Beims, in preparation (2010).
- [33] R. Klages, *Microscopic chaos, fractals and transport in nonequilibrium statistical mechanics* (World Scientific, 2007).
- [34] G. Casati, C. Mejía-Monasterio, and T. Prosen, *Phys. Rev. Lett.* **101**, 016601 (2008).